

# The Quasi Two-Day Wave - The Results of Numerical Simulation with the COMMA - LIM Model

K. Fröhlich, C. Jacobi, M. Lange and A. Pogoreltsev

## Summary

The quasi two-day wave (QTDW), a prominent feature of the mesosphere mainly around solstices, is simulated with the COMMA-LIM Model (Cologne Model of the Middle Atmosphere - Leipzig Institute for Meteorology). The calculations are made approximately one month after the summer solstice in the Northern Hemisphere when the QTDW reaches its maximum in the mesosphere and lower thermosphere. The results show that the QTDW produces a moderate westward forcing of the zonally averaged flow and a poleward driving of the residual mean meridional circulation.

## Zusammenfassung

Die Quasi Zwei-Tage Welle (QTDW), eine deutliche Erscheinung in der Mesosphäre kurz nach dem Sommer Solstitium, wird mit dem COMMA-LIM Modell (Cologne Model of the Middle Atmosphere - Leipzig Institute for Meteorology) simuliert. Die Zwei-Tage Welle wurde unter Juli-Bedingungen an der unteren Modellgrenze angeregt, zu der Zeit, zu der sie ihr Maximum in der Mesosphäre und unteren Thermosphäre erreicht. Die Ergebnisse zeigen eine sich westwärts ausbreitende Welle, die auf den Grundstrom eine moderate Beschleunigung nach Westen ausübt. Die residuelle mittlere Meridional Zirkulation erfährt dadurch eine zum Pol gerichtete Triebkraft.

## 1 Introduction

The quasi two-day wave (QTDW) has been observed in the upper stratosphere and mesosphere from the ground and from space over the past 25 years (e.g., *Muller and Nelson, 1978; Kalchenko, 1987; Plumb, 1987; Jacobi et al., 1997; Liebermann, 1998; Gurubaran et al., 2001*). The wave occurs with greatest amplitudes after summer solstice in both hemispheres and lasts for a few weeks. It propagates westward with a zonal wavenumber 3, also observed is wavenumber 4 (*Rodgers and Prata, 1981; Meek et al., 1996*) and periods close to 48 hours in the Southern Hemisphere (e.g., *Plumb, 1987*) and 50-52 hours in the Northern Hemisphere (e.g., *Muller, 1972*). As a characteristic feature, partially in the Southern Hemisphere and at low latitudes the meridional wind disturbance appears 2 to 3 times larger than the zonal wind (*Gurubaran et al., 2001*) whereas Jacobi (1997) reports that a ratio of the zonal to meridional wind amplitude is of about unity at 52° N. Typical amplitudes of the meridional wind disturbance  $v'$  are shown with 20 -30 m/s (*Gurubaran et al., 2001*). There is also a signal in the temperature field from satellite measurements with disturbances between 0.4 and 0.6 K (*Rodgers and Prata, 1981*). The latitudinal structure of the QTDW in the temperature oscillations shows maximized amplitudes near 20° (*Randel, 1994*) in each hemisphere.

Two mechanisms of excitation are in discussion: Salby (1981) proposes the QTDW as a manifestation of the Rossby-gravity normal mode with wave number 3 which corresponds to an eigenfunction of Laplace’s tidal equation. Another suggested forcing of the QTDW is a development of the baroclinic instability near the summer stratospheric wind jet (*Plumb, 1987; Pfister, 1985*), whereas Randel (1994) proposes the QTDW-appearance as a combination of resonant and unstable modes.

The spontaneous excitation of the QTDW succeeded only with some GCM’s (e.g., *Hunt, 1981; Norton and Thuburn, 1996, 1997*). It is possible that the lack of small scale perturbations at the model boundary of mechanistic models may hinder the excitation of an instability (*Palo et al., 1999*). But independently from its origin, the study of propagation and interaction of the wave with the mean flow, tides and solar variability is possible with mechanistic models through external forcing. This is the main task of this paper.

In the second section a short description of the model setup used for the simulation is given. In the third section the influence of the QTDW on zonally averaged circulation is discussed using time-space analysis and the Eliassen-Palm (EP) flux diagnostics. The residual mean meridional circulation will be also estimated. In the conclusion the main results are summarized.

## 2 Model Setup

The *Cologne Model of the Middle Atmosphere* (COMMA) is a three-dimensional global mechanistic model of the Earth’s atmosphere from approximately 3 km to 135 km in logarithmic pressure heights with 24 layers (at this time in the Leipzig version) and a horizontal resolution of 64 gridpoints in longitude and 36 in latitude.

The model contains a full description of radiative processes. It simulates the circulation in the middle atmosphere and enables investigations of tides, planetary waves and change of radiative forcing through atmospheric constituent changes. For more information the reader is referred to Lange (2001) and references therein.

To force the QTDW the Hough function for the (3,0) normal atmospheric mode is calculated (*Swarztrauber and Kasahara, 1985*). The latitudinal structure of the wave number 3 Rossby mode  $F(\phi)$  at the lower boundary in the geopotential field was included in the forcing equation

$$h(\lambda, \phi, t) = (1 - \exp(-\frac{t}{\tau})) F(\phi) \cos(3\lambda - \omega t). \quad (1)$$

Here,  $\lambda$  refers as longitude,  $\phi$  as latitude and  $\omega$  as the periode. With  $\tau = 259200$  s (3 days) the forcing reaches 95% of its amplitude in approximately 9 days. The period of the forcing remains constant with 51.5 hours during the simulation. This period was found as the one with the strongest model response. The maximum of the amplitude at the lower boundary was set to 30 geopotential meters.

After 40 days of settling time for the general circulation with the QTDW a period of 17 days was recorded to investigate the phenomenon. To estimate the influence of the QTDW on the zonally averaged circulation a reference run was performed without the QTDW forcing.

### 3 Results

The characteristic properties of the middle atmosphere in zonal wind during summer are the mesospheric easterlies which extend up to the mesopause where the wind reverses and becomes westerly. This is shown in Figure 1 (top and middle). There are two peaks in the easterlies, one at the equator and one at  $40^\circ$  N at 45 km. In the winter hemisphere westerlies dominate up to approximately 95 km and the maximum peaks at 55 km at roughly  $70^\circ$  S.

Considering the time averaged zonal mean wind field from the reference run (Fig.1, bottom) and the run with QTDW-forcing (Fig.1, top) the greatest differences occur at the stratopause southward of the equator. This is due to an easterly maximum at this height at the equator with velocities of approximately 35 m/s. Note that the circulation in the tropical stratosphere is not well expressed in COMMA-LIM, for example it contains no Quasi-Biennial Oscillation.

Another significant change is recognized as a tongue-shaped negative difference - an increase in absolute velocity - from  $10^\circ$  N at 60 km up to 100 km at approximately  $60^\circ$  N. It will be shown below that this tongue coincides with a westward momentum forcing due to the divergence of the Eliassen-Palm flux. In addition, below this tongue exists a similar structure of positive differences which means a negative acceleration of the zonal flow. Changes in the environment are possibly induced from the changed wind field, but they may also arise from filtering conditions for gravity waves.

#### Fourier Analysis

The structure of the QTDW is analyzed from the raw model results by using spatial and time Fast Fourier Transformation. The geopotential structure of the wave is shown in Figure 2. The structure extends from the mesosphere into the the lower thermosphere. The maximum of the geopotential field disturbance is found at midlatitudes of the Northern Hemisphere (NH) in the mesopause region where the zonal wind reverses.

Figure 3 shows the vertical and latitudinal structure of the QTDW in the zonal and meridional wind amplitude and temperature amplitude, respectively. As can be seen, the meridional wind component dominates the wind distortion in the mesosphere at midlatitudes. In high latitudes the magnitude of the two wind components becomes comparable. Although the wave is primarily a summer hemisphere phenomenon, the magnified values of the meridional wind extend into the winter hemisphere. The region of strongest amplitude values reaches from the equator at 65 km to the midlatitudes of NH at 85 km.

In accordance with Salby (2001) comparison of the geopotential field (Fig.2) with the temperature field (Fig.3, bottom) reveals that the temperature maxima of the QTDW occur at locations of sharp vertical changes in the geopotential height amplitude.

The lowest temperature maximum is found at  $25^\circ$  N in 55 km with 6.5 K while two maxima of similar magnitude at midlatitudes exist in 88 km and 115 km. These structures resemble to results of Palo (1999) who has found in calculations with GCM's and comparisons with satellite data; although they were carried out for the southern hemisphere.

These structures were then found as westward propagating fields (see Figure 4) by

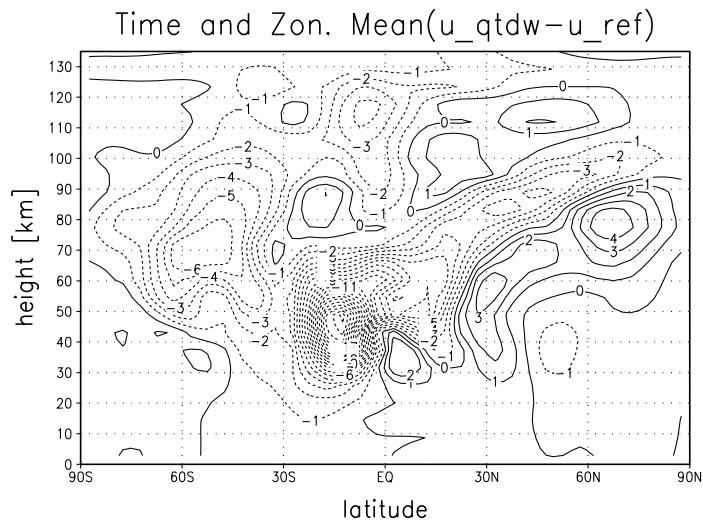
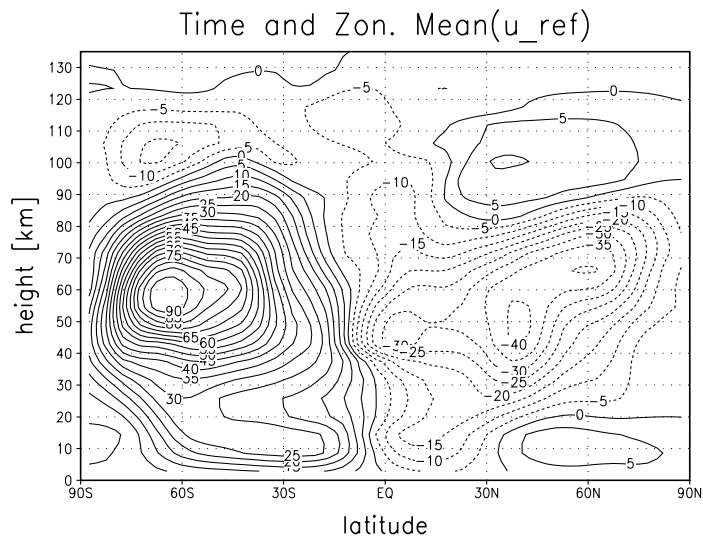
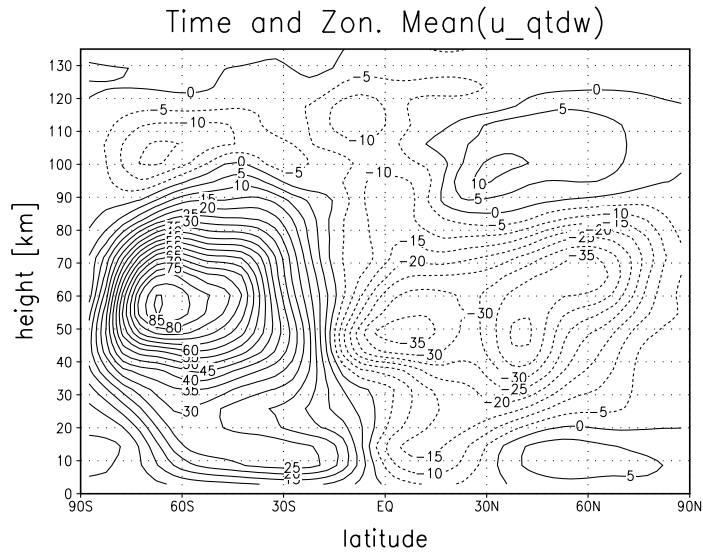


Figure 1: Zonal mean zonal velocity  $u$ . Top:  $u$  of the QTDW, middle:  $u$  of the reference run, bottom: difference between QTDW run and reference run; Mid-July conditions.

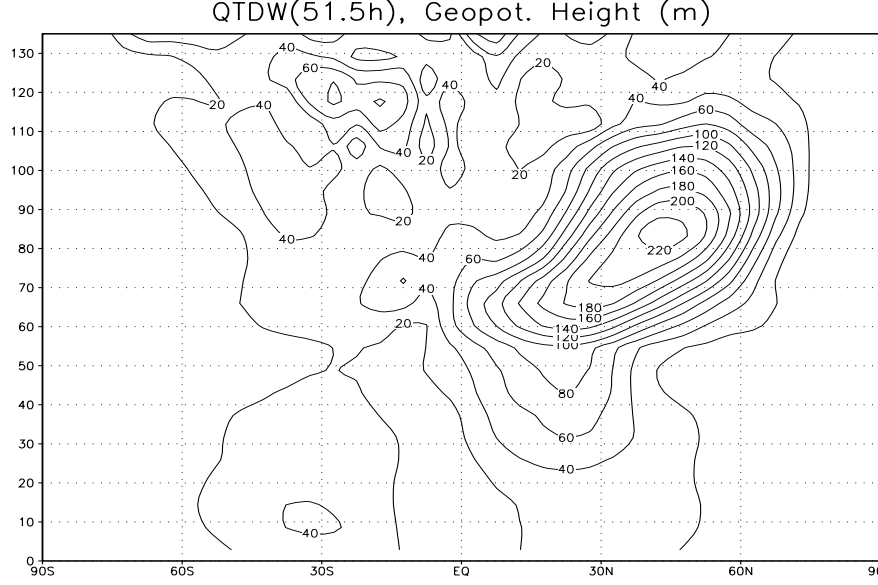


Figure 2: Amplitude of the Geopotential Height Perturbation of the QTDW (m) for Mid-July conditions.

using the formulas given in Hayashi (1971). His formulation allows to distinguish between amplitudes and phases of progressive and retrogressive waves applying cross-spectra analysis between the time dependent space-Fourier coefficients. Note that the eastward parts of the QTDW are negligible.

Horizontal motion of the QTDW at 90 km is mapped in Figure 5. The horizontal wind disturbance components  $u'$  and  $v'$  compose global-scale gyres that are centered near the equator. The strongest motion exists at northern midlatitudes but extend also into the southern hemisphere as far as  $40^\circ$  S. Salby (2001) shows a similar picture and determined a consistent pattern with observations.

### Wave-Mean Flow Interaction

To understand the wave-mean flow interaction of the QTDW it is useful to evaluate the wave Eliassen-Palm (EP) fluxes and their influences through the Transformed Eulerian-Mean (TEM) equations. The zonal TEM momentum equation in spherical coordinates can be written as follows (Andrews *et al.*, 1987):

$$\overline{u}_t + \overline{v}^* \left[ \frac{(\overline{u} \cos \phi)_\phi}{a \cos \phi} - f \right] + \overline{w}^* \overline{u}_z = \frac{1}{\rho_0 a \cos \phi} \nabla \cdot F, \quad (2)$$

with meridional and vertical EP flux components

$$F^\phi = \rho_0 a \cos \phi \left( \overline{u}_z \frac{\overline{v' \theta'}}{\overline{\theta}_z} - \overline{v' u'} \right) \quad (3)$$

and

$$F^z = \rho_0 a \cos \phi \left\{ \left[ f - \frac{1}{\rho_0 a \cos \phi} (\overline{u} \cos \phi)_\phi \right] \frac{\overline{v' \theta'}}{\overline{\theta}_z} - \overline{w' u'} \right\}. \quad (4)$$

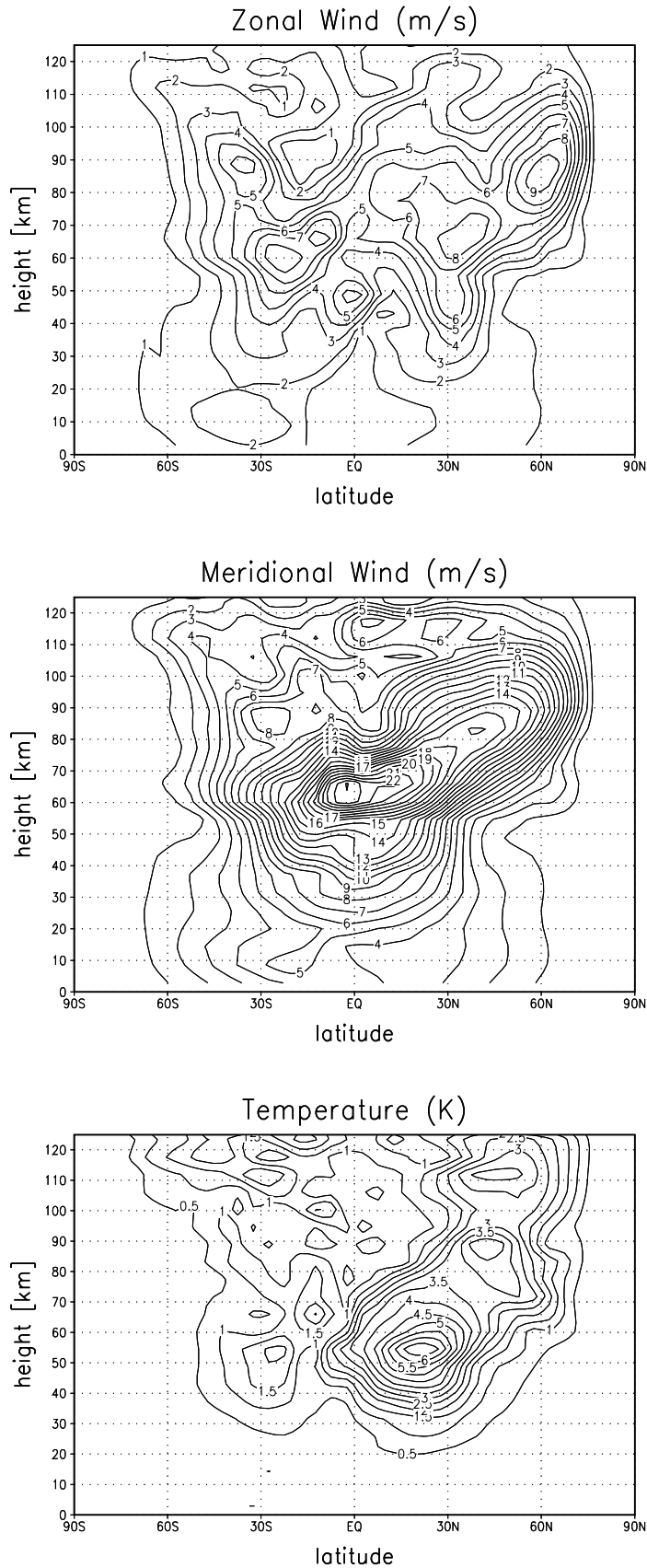


Figure 3: Amplitudes of the QTDW. Top: zonal wind  $u$  (m/s), middle: meridional wind  $v$  (m/s). Contour intervall is 1 m/s. Bottom: Temperature  $T$  (K), contour intervall is 0.5 K. Conditions like in Fig. 1.

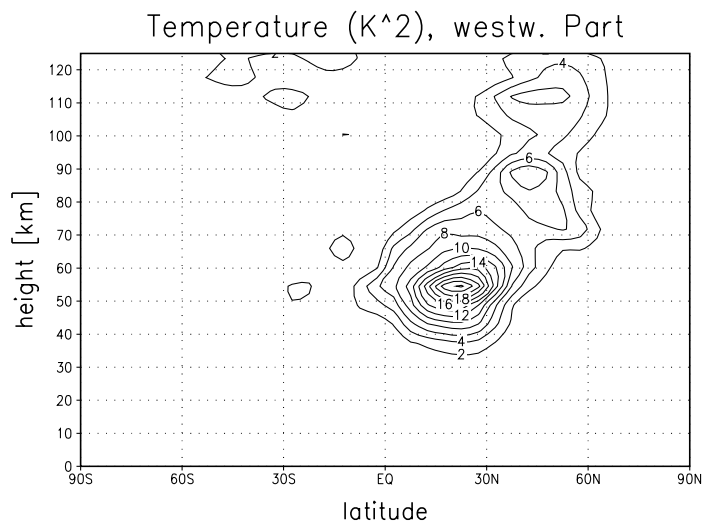
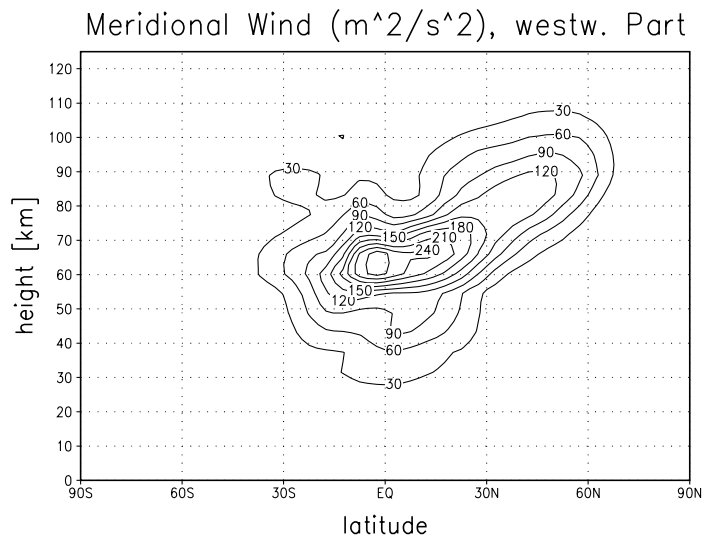
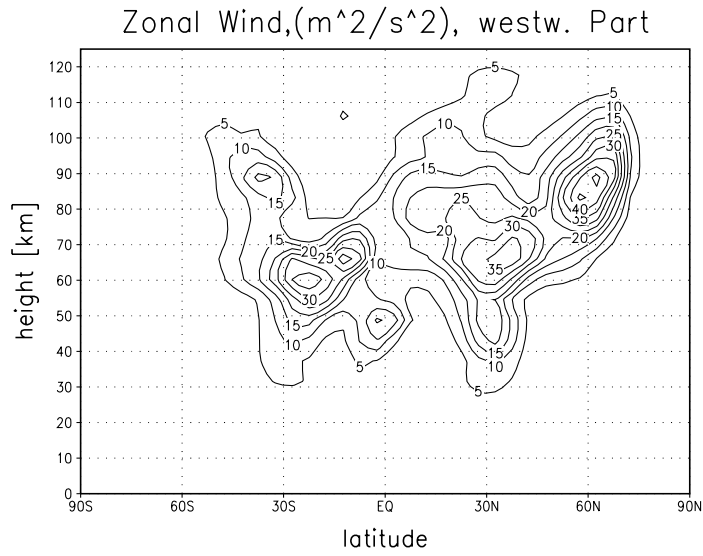


Figure 4: Westward propagating parts of the QTDW. Top: zonal wind  $u$ , middle: meridional wind  $v$ , bottom: temperature  $T$ .

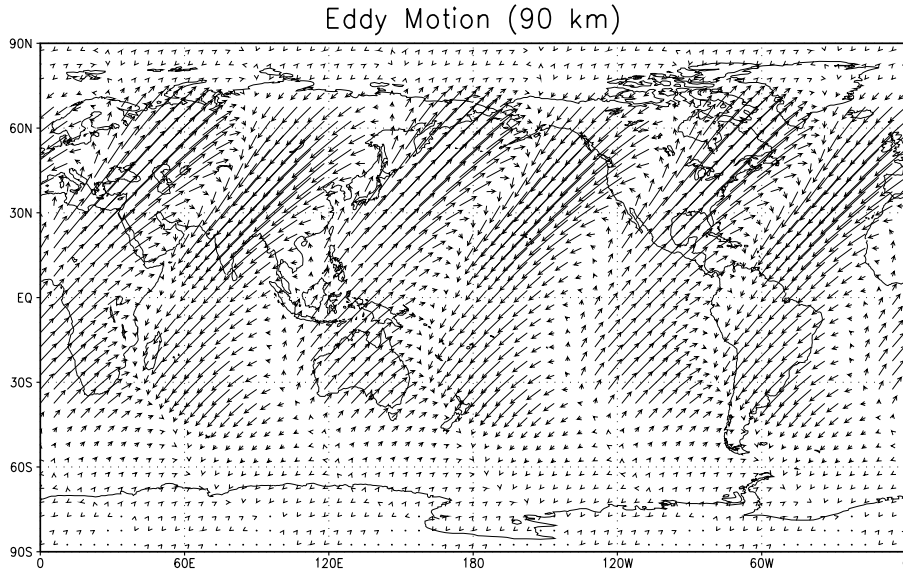


Figure 5: Eddy motions of the QTDW at 90 km.

Overbars and primes denote zonally averaged and perturbation quantities,  $a$  is the Earth's radius,  $\phi$  is latitude,  $f$  is the Coriolis parameter,  $\rho_0$  the density,  $\theta$  means the potential temperature and subscripts denote the corresponding derivatives. The residual mean meridional circulation ( $0, \bar{v}^*, \bar{w}^*$ ) has the components

$$\bar{v}^* = \bar{v} - \frac{1}{\rho_0} \frac{\partial}{\partial z} \left( \rho_0 \frac{\overline{v' \theta'}}{\partial z} \right) \quad (5)$$

$$\bar{w}^* = \bar{w} + \frac{1}{a \cos \phi} \frac{\partial}{\partial \phi} \left( \cos \phi \frac{\overline{v' \theta'}}{\partial z} \right). \quad (6)$$

Figure 6 shows the calculated force per unit mass due to the divergence of the Eliassen-Palm flux (EPFD), the vertical convergence of eddy heat transport  $(F^z)_z$  and the meridional convergence of eddy momentum flux  $(F^\phi)_\phi$ . The QTDW induces moderate westward forcing at the midlatitudes of the Northern Hemisphere in the mesosphere and lower thermosphere (MLT) region which can be seen in the top and middle of Fig.6. The separation reveals that this is due to the dominant vertical convergence of meridional heat flux  $(F^z)_z$ .

The eddy momentum flux divergence  $(F^\phi)_\phi$  exhibits an almost symmetric structure in the MLT region. In the NH between  $10^\circ$  and  $50^\circ$   $(F^\phi)_\phi$  accounts for weak eastward driving which is superposed by  $(F^z)_z$ , while particularly south of the equator westward acceleration appears in the winter hemisphere. The latter seems to be the reason for an increasing stratopause easterly jet above the equator (see also Fig.1).

The residual mean meridional wind  $\bar{v}^*$  in midlatitudes (Fig.7) is directed poleward because of the offset by Coriolis acceleration associated with downward residual motion  $\bar{w}^*$ .

At the high latitudes a weak cell of poleward transport exists above 95 km, implying downward motion at the pole and south- and upward transport below 90 km (Figure



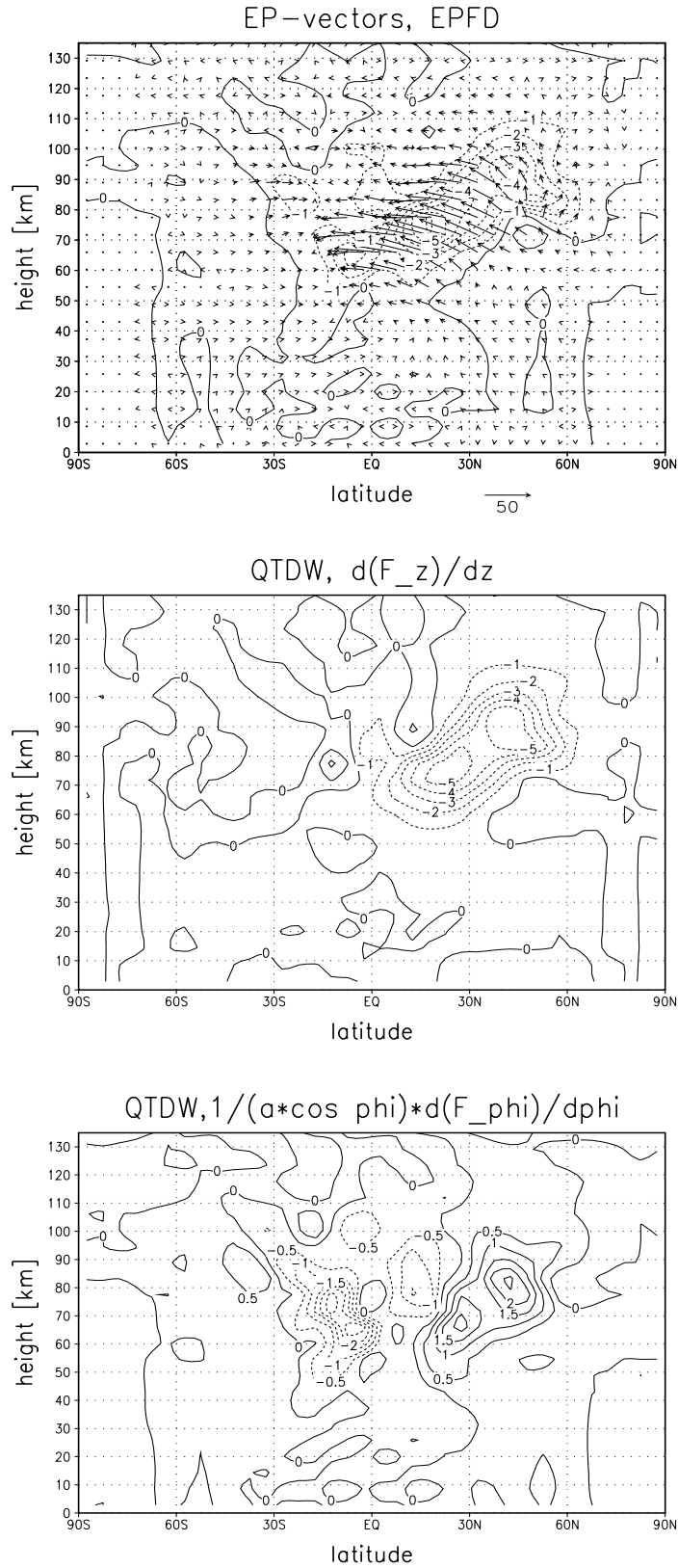


Figure 6: Top: the force per unit mass (contour lines  $1 \text{ ms}^{-1} \text{ day}^{-1}$ ) and EP-flux vector (arrows, the vertical component is scaled by factor 50), middle: vertical convergence of meridional heat flux per unit mass and day  $(F^z)_z$ , bottom: meridional convergence of momentum flux per unit mass and day  $(F^\phi)_\phi$ .

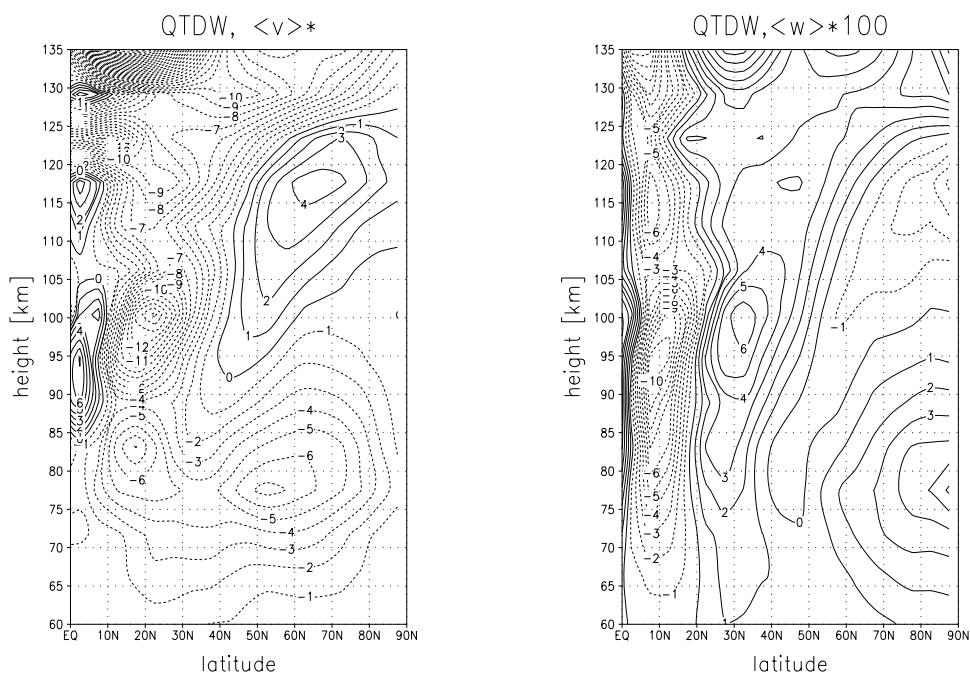


Figure 7: Residual mean meridional circulation of the mesosphere and lower thermosphere in Northern Hemisphere. left: meridional velocity  $\bar{v}^*$ ; right: vertical velocity  $\bar{w}^*$ , scaled with factor 100.

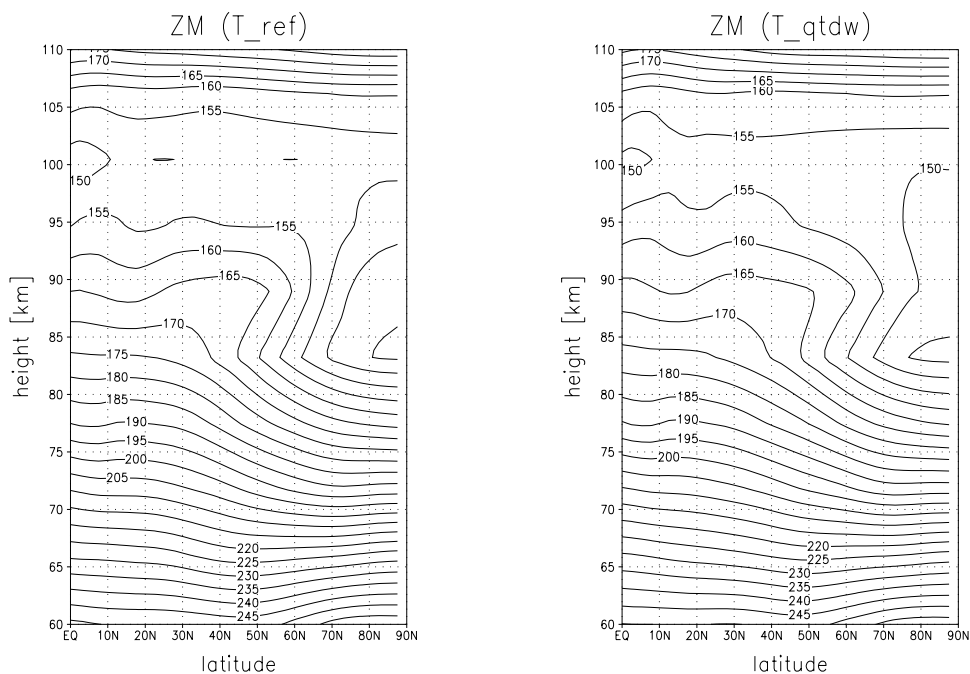


Figure 8: Time and zonally averaged Temperature of the mesosphere and lower thermosphere at Northern Hemisphere in July. left: reference run; right: run with QTDW-forcing.

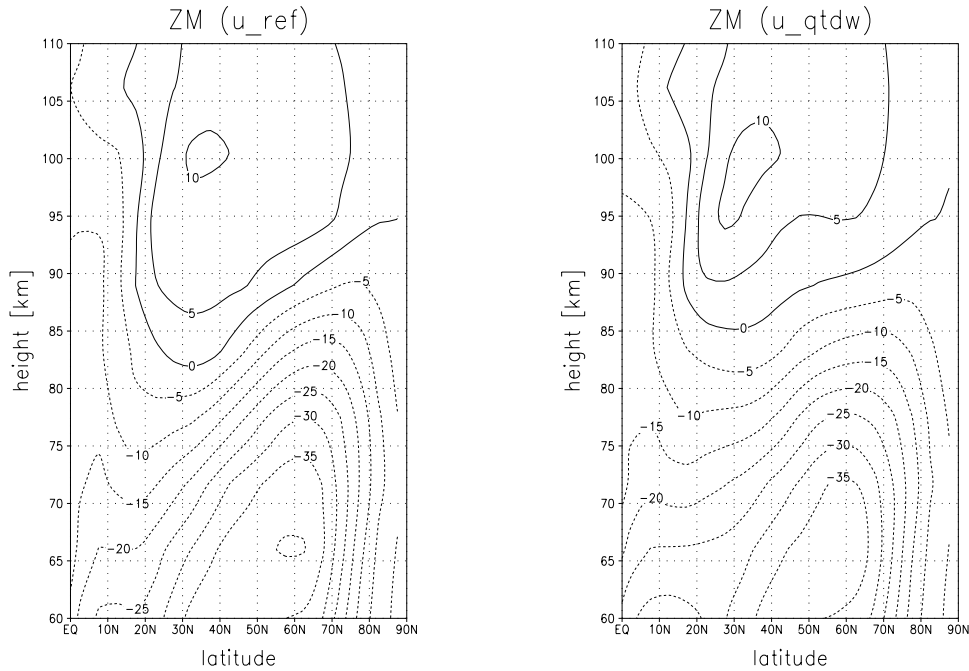


Figure 9: Time and zonally averaged Zonal Wind with the same localisation as in Fig. 8.

7). Lieberman (1999) reported a residual vertical mean circulation which results through upward/downward motion in a cool/warm pair of cells tilted across the middle and high Southern Hemisphere latitudes during summer conditions. It acts to reduce the meridional gradient of  $\bar{T}$  which in turn must lead, due to the thermal wind balance, to a decreasing vertical shear of the zonal wind. This feature appears also in the COMMA-LIM calculations (see Figure 8 and 9) for the NH summer.

## 4 Conclusions

The QTDW is simulated within the COMMA-LIM using external forcing at the lower boundary. The shape of the geopotential and meridional wind field are in a good agreement with other investigations of the QTDW. The wave is identified as a westward propagating phenomenon with the aid of cross spectrum analysis. The EP flux divergence per unit mass shows an westward acceleration of the mean flow in a broad region of the summer MLT up to  $5 \text{ m s}^{-1} \text{ day}^{-1}$ . This driving is due to the vertical convergence of the meridional heat flux. The residual mean meridional circulation indicates at mid and high latitudes an poleward residual  $\bar{v}^*$ .

The residual meridional mean circulation acts to reduce the pole-equator gradient of the mean Temperature at 90 km and so the vertical shear of the zonal mean wind decreases.

## References

- Fritts, D. C., Isler, J. R., Mean Motions and Tidal And Two-Day Structure and Variability in the Mesosphere and Lower Thermosphere over Hawaii. J. Atmos. Sci., 1994, pp.2145–2164

- Fritts, D. C., Isler, J. R., Lieberman, R. S., Burrage, M. D., Marsh, D. R., Nakamura, T., Toshihata, T., Vincent, R. A. and Reid, I.M.,  
Two-day wave structure and mean flow interactions observed by radar and High Resolution Doppler Imager. *J. Geophys. Res.*, 1999, D4, pp. 2953-3969
- Gurubaran, S., Sridharan, S., Ramkumar, T. K. and Rajaram, R.  
The mesospheric quasi-2-day wave over Tirunelveli 8.7° N. *Journal of Atmospheric and Solar Terrestrial Physics*, 2001, No. 63, pp. 975-985
- Hagan M. E., Forbes, J. M. and Vial, F. Numerical Investigation of the propagation of the Quasi-Two-Day Wave Into the Lower Thermosphere,  
*J. Geophys. Res.*, 1993, D12, pp. 23193-23205
- Jacobi, C., Schminder, R., and Kürschner, D., The quasi 2-day wave as seen from D1 LF wind measurements over Central Europe (52° N, 15° E) at Collm. *J. Atmos. Solar-Terr. Phys.* 59, 1997, pp. 1277-1286
- Kalchenko, B.V., Characteristics of atmospheric disturbances with a quasi 2-day period. *Handbook for MAP 25*, pp. 112-118
- Lange, M., Modellstudien zum  $CO_2$ -Anstieg und  $O_3$ -Abbau in der mittleren Atmosphäre und Einflußs des Polarwirbels auf die zonale Symmetrie des Windfeldes in der Mesopausenregion. *Wiss. Mitt. d. Instituts f. Meteorologie Leipzig*, 2001, Bd 25
- Liebermann, R., Eliassen-Palm Fluxes of the 2-day Wave, *J. Atmos. Sci.*, 1999, pp. 2846-2861
- Meek, C. E., Manson, A. H., Franke, S. J., Singer, W., Hoffmann, P., Clark, R. R., Tsuda, T., Nakamura, T., Tsutsumi, M., Hagan, M., Fritts, D. C., Isler J. and Portnyagin, Yu I., Global study of northern hemisphere quasi-2-day wave events in recent summers near altitude. *J. Atmos. Solar-Terr. Phys.* 58, 1996, pp. 1401-1411
- Muller, H. G., Long period wind oscillations. *Phil. Trans. Roy. Soc.* A727, pp. 585 - 598
- Muller, H. G. and Nelson, L., A travelling quasi 2-day wave in the meteor region, *J. Atmos. Terr. Phys.*, 40, 1978, pp. 1851 - 1861
- Norton, W. A. and Thuburn, J., The two-day wave in a middle atmosphere GCM. *Geophys. Res. Lett.*, 1996, No.23, pp. 2113-2116
- Norton, W. A. and Thuburn, J., Sensitivity of mesospheric flow, planetary waves, and tides to strength of gravity wave drag, *J. Geophys. Res.*, 1999, D24, pp. 30897-30911
- Palo S. E., Roble, R. G. and Hagan, M. E., TIME-GCM Results for the Quasi-Two-Day Wave, *Geophys. Res. Lett.*, 1998, pp. 3783-3786
- Palo S. E., Roble, R. G. and Hagan, M. E., Middle atmosphere effects of the Quasi-two-day wave determined from a General Circulation Model, *Earth Planets Space*, 1999, pp. 629-647
- Pfister, L., Baroclinic Instability Jets with Applications to the Summer Mesosphere, *J. Atmos. Sci.*, 1985, pp. 313-330
- Plumb, A., Baroclinic Instability of the Summer Mesosphere: A Mechanism for the Quasi-Two-Day wave?. *J. Atmos. Sci.*, 1983, pp. 262-270
- Plumb, A., Vincent, R. A. and Craig, R. L., The Quasi-Two-Day Wave Event of January 1984 and its Impact on the Mean Mesospheric Circulation, *J. Atmos.*

- Sci., 1987, pp. 3030-3036  
Randel, W. J., Observations of the 2-day Wave in NMC  
Stratospheric Analyses, J.  
Atmos. Sci., 1994, pp. 306-313
- Rodger, C. D. and Prata, A. J., Evidence for a Traveling Two-day Wave in the  
Middle Atmosphere, J. Geophys. Res., 1981, pp. 9661-9664
- Salby, M.L., The 2-Day Wave in the Middle Atmosphere: Observations and Theorie.  
J. Geophys. Res., 1981, pp. 9654-9660
- Salby, M.L., Callaghan, P.F., Seasonal Amplification of the 2-Day Wave: Relationship  
between Normal Mode and Instability. J. Atmos. Sci., 2001, Vol. 58, pp. 1858-  
1868
- Swartztrauber, P. N. and Kasahara, A., The vector harmonic analysis of Laplace's  
tidal equations. SIAM, J. Sci. Stat. Comput. 6, 1985, pp. 464 - 491
- Walterscheid, R. L. and Vincent, R. A., Tidal generation of the phase-locked 2-day  
wave in the southern hemisphere summer by wave-wave interactions, J. Geophys.  
Res., 1996, pp. 26567-26576